Multi-Area Reserve Dimensioning using Chance-Constrained Optimization

Anthony Papavasiliou, *Senior Member, IEEE,* Alberte Bouso, Senad Apelfröjd, Ellika Wik, Thomas Gueuning, Yves Langer

***Abstract*—We propose a chance-constrained formulation for the problem of dimensioning frequency restoration reserves on a power transmission network. We cast our problem as a two-stage stochastic mixed integer linear program, and propose a heuristic algorithm for solving the problem. Our model accounts for the simultaneous sizing of both upward and downward reserves, and uncertainty driven by imbalances, contingencies and available transmission capacity. Our core methodology is further adapted in order to minimize inter-zonal flows and in order to split reserve requirements between automatic and manual frequency restoration reserves. We apply our methodology to the problem of sizing reserves in the four load frequency control areas of the Swedish power system. We demonstrate the benefits of our method in terms of decreasing reserve requirements in the absence of reserve sharing, we analyze the spatial allocation of reserves, and we perform various sensitivity analyses.**

***Index Terms*—Reserve requirements, multi-area reserve sizing, probabilistic dimensioning, reserve deliverability, chance constraints, probabilistic constraints**

I. Introduction

A. Motivation

As European electricity markets are becoming increasingly coupled, there is a thrust for the closer coordination of transmission system operators (TSOs) in the procurement of reserve capacity and the activation of real-time balancing energy. This is reflected in numerous initiatives, including the launch of pan-European platforms for balancing close to real time using frequency restoration reserves (the MARI and PICASSO platforms), as well as the coordinated international trade of reserve capacity in the pan-European day-ahead electricity market (articles 40-42 of the Electricity Balancing Guideline of the European Union [1]).

The coordination of real-time dispatch of balancing energy from frequency restoration reserves, which is the objective of these initiatives, is inevitably linked to the constraints of the transmission network. This relates to both (i) the delivery of energy from reserve resources in real time, as well as (ii) the procurement of reserves in forward (e.g. day-ahead) reserve markets in a way that anticipates congestion patterns in the power transmission network, so that reserves are not only procured in the appropriate quantities, but also at the appropriate locations. The latter problem is referred to as reserve deliverability [2], [3], and generalizes the problem of reserve sizing[1] to a multi-area setting. Our work is concerned with framing and tackling this problem in the context of recent evolutions in the institutional requirements of European electricity markets.

Recent European legislation[2] dictates the fundamental criterion for dimensioning reserves in article 157 of the System Operation Guideline (SOGL) of the European Union [4]. This criterion is system reliability, as indicated in paragraphs (h) and (i) of article 157:
"*all TSOs of a LFC block shall ensure that the positive [resp. negative] reserve capacity on FRR or a combination of reserve capacity on FRR and RR is sufficient to cover the positive [resp. negative] LFC block imbalances*[3] *for at least 99 % of the time*".

The probabilistic requirements dictated by the SOGL have motivated considerable research on probabilistic dimensioning methods [5]. The general idea of such methods is to collect historical data of system imbalances, and set reserve requirements to the quantile of the imbalance distribution that corresponds to the target reliability of the system.

The basic methodology can be enhanced with various features. (i) Contingencies[4] can be incorporated, typically by assuming that they are independent of so-called normal imbalances. One can then compute the convolution of the capacity outage probability table of the system [6] with the distribution of normal imbalances and size reserves by selecting the appropriate quantile of this newly computed distribution. (ii) Reserves can be dimensioned dynamically by adapting the uncertainty distribution of the system to observable day-ahead conditions, such as load forecasts, wind forecasts, demand forecasts, 15-minute interval of the day (in order to capture ramps in unit schedules on the change of the hour), and a number of other explanatory factors which are referred to as *imbalance drivers*. One can then use machine learning methods such as k-means [5], k-nearest-neighbors [7] or artificial

Anthony Papavasiliou is with Center for Operations Research and Econometrics, Université catholique de Louvain and N-SIDE; Email: anthony.papavasiliou@uclouvain.be, apa@n-side.com; Phone: +32 10 474325. Alberte Bouso, Thomas Gueuning and Yves Langer are with N-SIDE. Senad Apefröjd and Ellika Wik are with Svenska kraftnät.

[1]We refer to reserve sizing interchangeably as reserve dimensioning, or quantifying reserve requirements.

[2]More generally, Part IV of the System Operation Guideline on load frequency control and reserves addresses the dimensioning of reserves: articles 153-156 focus on frequency containment reserve (FCR), articles 157-159 address frequency restoration reserve (FRR), articles 160-162 are dedicated to replacement reserve (RR), and articles 163-170 address reserve sharing within a synchronous area.

[3]The imbalance per LFC area used in this work is the open-loop area control error (ACE).

[4]System imbalance is typically the result of contingencies and normal imbalances. Contingencies refer to unplanned outages of power system components. Instead, normal imbalances are related to continuous sources of uncertainty, such as forecast errors.

neural networks [8] in order to compute the target quantile, which translates to the appropriate reserve requirement for the following day, in a way that is adapted to the observable day-ahead system conditions. This methodology has been adopted by the Belgian transmission system operator [9], and is operational in Belgium since February 2020.

Although the aforementioned methodologies adequately address the probabilistic requirement for reserve dimensioning that is dictated by SOGL in the absence of transmission network constraints, there are scant efforts [10] in extending these methodologies in the presence of transmission network constraints. This creates a methodological gap in the existing literature, especially in light of the fact that European legislation foresees two principal means of reserve sharing between different operating areas, which are referred to respectively as *exchange* and *sharing* of balancing capacity[5]. Reserve *exchange* refers to the practice whereby a system operator can procure its own reserve needs from a neighboring control area through exclusive access to the reserve in question. In reserve *sharing*, TSOs operating neighboring control areas gain non-exclusive access to the same reserves, counting on the fact that the two system operators will not require the same resource simultaneously. This is a stronger form of interaction than exchange, and it aims at correspondingly higher reductions in reserve requirements. The concept that we describe in this paper is rather akin to reserve sharing.

B. Nordic Context

In response to the aforementioned evolutions in EU legislation [4] and given the intention of the Nordic countries (Sweden, Norway, Finland and Denmark) to increase coordination in the commitment and deployment of frequency reserves (fast frequency reserve, FCR and FRR), the Nordic system operators[6] put in place the Nordic System Operation Agreement (SOA) [11], as well as more specific provisions for the management of reserves in the synchronous area proposals [12], [13]. In relation to our analysis, we isolate the following principles that are set out in these agreements: (i) Each TSO is responsible for FRR dimensioning for its own control area in accordance with the frequency restoration reserves (FRR) dimensioning methodology specified in the SOA (i.e. a probabilistic criterion). (ii) The dimensioning shall be applied on no less than one year of historical data.

There are a number of implications from these requirements for our analysis. (i) The first implication is that our analysis focuses on two types of FRR: automatic FRR (aFRR) and manual FRR (mFRR). aFRR is akin to automatic generation control, i.e. reserves that follow the dispatch signal of an automatic controller which adjusts setpoints every few seconds. aFRR is required to obey a full activation time of a few (e.g. five) minutes. mFRR is akin to contingency reserves, and is required to obey a full activation time of no more than 15 minutes, which is the reference time step for real-time balancing operations in Europe. Our target methodology aims at sizing each of these reserve types, while accounting for their interactions, as explained further in section III-C. (ii) The second implication is that our methodology is required to exploit at least one year of historical data that are relevant for the sizing of reserves, and that normal imbalances, contingencies and transmission capacity uncertainty should be accounted for by our methodology. As indicated in Fig. 1, the Nordic load frequency control (LFC) block contains eleven LFC areas (SE1-SE4, NO1-NO5, DK2, FI), where LFC areas correspond also to bidding zones, and four control areas (Sweden, Norway, Denmark, Finland), where control areas correspond to each TSO area. Our analysis will focus on reserve sharing within the Swedish control area, with the goal being to share reserve between the four LFC areas (SE1-SE4) of the Swedish control area. Note, nevertheless, that the methodology that we set forth in this work can be extended to the sizing of reserves throughout the entire Nordic LFC block, as we discuss in section V.

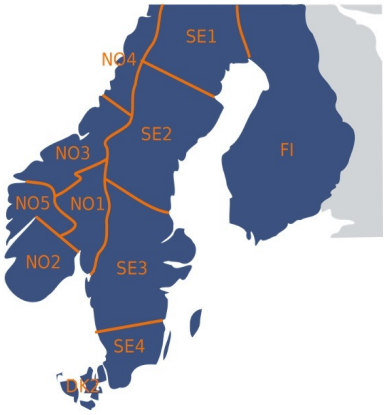

Fig. 1. The Nordic LFC block consists of four control areas (Sweden, Norway, Denmark, and Finland) and eleven LFC areas. Our work is concerned with the four Swedish LFC areas, SE1 - SE4.

C. Multi-Area Reserve Dimensioning in the Literature and in Practice

Although probabilistic constraints[7] in the context of reserve sizing and the presence of networks have been considered extensively in the academic literature, our understanding of the state of the art reveals a methodological gap in terms of formulating the problem in a way that is aligned with the SOGL requirements. We proceed to discuss in further detail some of the work that is related to our context.

The decomposition method is a recursive method for estimating reliability in systems with network constraints that is proposed in the classical reliability literature [15]. Although the method can be applied for assessing reliability for systems with *given* reserve capacities, scalability is a challenge, and it

[5]Balancing capacity is the European terminology for reserve, and the two terms are used interchangeably in the present work.

[6]Sweden, Norway, Finland and Denmark are represented by Svenska kraftnät, Statnett, Fingrid, and Energinet respectively. Note that the dimensioning and coordination of reserves is the sole responsibility of transmission system operators (TSOs), subject to the supervision of the competent regulatory authorities.

[7]Note that, following [14], we use the terms *probabilistic constraints* and *chance constraints* interchangeably.

is unclear how the method can be employed for endogenously determining these reserve capacities.

The exchange and sharing of reserve capacity in the context of SOGL is discussed explicitly by De Haan [16]. The analysis is focused on the benefits of reserve sharing in Central Western Europe. However, in order to quantify these benefits the authors merge imbalances in different control areas, therefore one can conclude that transmission constraints are ignored in the analysis.

Regarding the aforementioned literature on deliverability, early research in this direction [2] is out of scope, since it focuses on scheduling units *given* zonal reserve requirements, or focuses on intra-zonal congestions [17] whereas the focus of the present paper is on inter-zonal congestions. In [18], the authors aim at correcting zonal reserve requirements, however without an explicit consideration of a probabilistic reliability criterion. Similarly, in [3] the authors consider the endogenous multi-area sizing of reserves, however without an explicit consideration of a probabilistic reliability criterion. The motivation in [10] is closest to our own work, in the sense of endogenously defining reserve requirements with an explicit consideration of a probabilistic reliability criterion and a consideration of transmission network limits. The idea of the authors is to employ empirical distributions of normal imbalances and contingencies in order to infer the exposure of zones to power shortfalls and inter-zonal lines to overloading. However, the authors employ a number of approximations in their approach, and do not consider the simultaneous interaction between the exchange of balancing energy between zones and the flow that this specific exchange implies on inter-zonal links.

Similarly to the case of the reserve deliverability literature, there exists a strand of literature related to our work which accounts for transmission network constraints while focusing on the scheduling or re-dispatch of *individual* resources in the system. Notable work that accounts simultaneously for chance constraints and transmission includes [19] and [20], although the methods are tied to specific distributions and treat aFRR capacity differently than the present work. A similar unit-based formulation is presented in [21], although the formulation is not targeted at satisfying a chance constraint but rather a robust operation criterion. Multi-area stochastic unit commitment methods [22] follow a similar structure: they consider the problem of scheduling each unit in the system, without directly tackling the question of endogenously determining the amount of reserve. These models thus require an excessive amount of input data, and introduce unnecessary computational complexity given the task at hand. Moreover, stochastic unit commitment models overlook the probabilistic reliability criterion of SOGL, and rather focus on balancing the cost of operation against the cost of failing to serve load.

The approach that we inspire ourselves from is the explicit representation of probabilistic constraints using binary indicator variables, as presented in [23]. Whereas the authors consider an application related to probabilistically constrained unit commitment, we present a formulation that applies to reserve dimensioning, and that captures the spirit of the requirement in SOGL.

It is further interesting to note that European system operators do not provide clear paths for multi-area probabilistic dimensioning. The French, Belgian, and German TSOs, for instance, document advanced methodologies for dynamic dimensioning [9], as well as the splitting of FRR capacity between aFRR and mFRR [24]. Nevertheless, it is not evident that there is a clear path for generalizing these methods, which are fundamentally based on the direct manipulation of density functions, to the case of network constraints.

D. Contributions and Organization of the Paper

We summarize the contributions of our work as follows:

Modeling. We present a novel methodology for dimensioning reserves according to a probabilistic criterion that is compliant with EU legislation while accounting for transmission network constraints. The framework that we propose breaks from the traditional approach that is advanced in EU practice of manipulating probability density functions and computing their quantiles, which is not adequate for FRR dimensioning in a multi-area context, and is rather based on mathematical programming. Our mixed integer programming formulation is highly flexible and extensible: it can simultaneously consider upward and downward reserve requirements, uncertainty in the form of normal imbalances, contingencies, and uncertain transmission capacities, and can be extended to consider additional features such as minimum zonal reserve requirements or limits on inter-temporal variations of reserve requirements.

Methodology. We propose a heuristic algorithm for resolving our chance-constrained model, which is computationally tractable and exact in certain cases. We adapt our methodology in order to size aFRR and mFRR capacity separately, while accounting for their interactions. We further adapt our methodology in order to allocate reserves in a way that limits unnecessary use of the transmission network.

Application. The framework that we present is intended for operational deployment, and results from a collaborative effort between Swedish TSO Svenska kraftnät and N-SIDE. We demonstrate that our proposed model and solution approach are capable of tackling one year of one-minute historical data which corresponds to up to 70,272 scenarios. In accordance with SOGL requirements, we use historical data from the Swedish grid in order to propose locational reserve requirements for each of the four Swedish areas. Our algorithm executes within minutes, and can also be executed by open-source solvers within acceptable run time. The resulting sizing decision can capture 76.1% (downward reserve) - 77.7% (upward reserve) of the potential savings that could be achieved by reserve sharing in the absence of transmission constraints.

In section II we motivate the benefits of multi-area dimensioning through an illustrative example, and provide indications of why the problem is challenging. We then formulate the problem at hand as a chance-constrained optimization, which is expressed as a two-stage stochastic mixed integer linear program. Section III outlines our proposed heuristic for solving the resulting stochastic program, a two-step procedure for sizing so as to minimize inter-area flows resulting from balancing actions, and adaptations to the basic problem that are

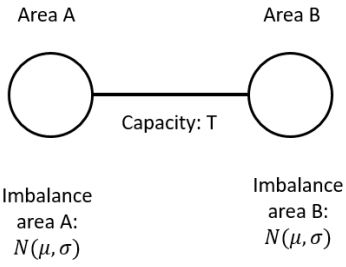

Fig. 2. A two-area system for motivating the problem of multi-area reserve dimensioning.

required for splitting total reserve capacity between aFRR and mFRR. Section IV presents an application of our approach to the problem of sizing reserves for the Swedish power system. Section V summarizes the contributions of the paper and presents areas of future research.

II. Problem Formulation

A. Motivating Example

In order to motivate the benefits of reserve sharing, the problem that we aim at solving, and how it is different from previous work considered in the literature, consider the motivating example of Fig. 2. We limit our attention to upward reserve, and use the convention that negative imbalance corresponds to a shortage of power.

Sizing in a single area. Let us first focus on area A, and assume that this area experiences imbalances that obey a normal distribution with a mean of $\mu = 0$ MW and a standard deviation of $\sigma = 100$ MW. Suppose that the reliability target defined by the TSO is $R = 99.9\%$. Then a probabilistic sizing methodology would require reserves R to be such that $\mathbb{P}[-Imb \leq r] = R$, which implies $r = \mu + \sigma \cdot \Phi^{-1}(R) = 309$ MW. Here, Imb is the imbalance of area A, r is the amount of reserve that the area carries, and Φ^{-1} is the inverse cumulative distribution function of the standard normal distribution.

Sizing in two areas: no reserve sharing ($T = 0$). Now consider a neighboring area with an identical and independent distribution of imbalances[8]. The two areas are assumed to be interconnected with a link that has a capacity T, as indicated in Fig. 2. It is already interesting to reflect on what a reliability target R implies for a two-area system. Concretely, one might interpret this goal in two different ways: (i) each area *separately* satisfies a reliability level R (i.e. a reliability requirement per LFC area), or (ii) the two-area system satisfies a reliability level R (i.e. a reliability requirement per control area). We adopt the second interpretation, following the SOGL requirement [4] and Nordic agreements [11], [12], [13]. Following the second interpretation, we can compute the required reserve for each area when the areas are fully isolated, i.e. when $T = 0$. Given the symmetry of the system, we can assume that the areas carry the same amount of reserve $r_A = r_B = r$, which implies $\mathbb{P}[max(-Imb_A, -Imb_B) \leq r] = R \Rightarrow \mathbb{P}[-Imb_A \leq r]^2 = R \Rightarrow r = \Phi^{-1}(\sqrt{R}) = 329.1$ MW per area (not 309 MW, as would be the case for interpretation (i)). Thus, the total reserve carried in the system is 658.2 MW. The first equality follows from the independence of the imbalance distributions. Note that the total reserve capacity is more than double the reserve of the previous paragraph. This is in line with the methodology that is presently applied by the French, German, and Belgian TSOs [24] for their respective control areas[9].

Sizing in two areas: copperplate ($T = +\infty$). If the two control areas can merge their imbalances, and assuming that the link has unlimited capacity $T = +\infty$, the overall system imbalance would be distributed (due to independence) according to $N(2 \cdot \mu, \sqrt{2} \cdot \sigma)$. Thus, the reserve requirement for the joint area is $r = 2 \cdot \mu + \sqrt{2} \cdot \sigma \cdot \Phi^{-1}(R) = 437$ MW. Effectively, by merging their imbalances, the two areas decrease their reserve requirement dramatically. The source of the savings is that the imbalances of each area can cancel each other out[10], and in a sense perform the same function as reserves. This is the intended benefit of reserve sharing, however the methodology completely overlooks the limited ability of the network to carry balancing energy.

Sizing in two areas subject to a transmission constraint ($0 < T < +\infty$). We now consider what would happen if the transmission line can only carry T MW in each direction. Given a realization Imb_z of imbalance in each area z, in order for these imbalances to be covered the two areas need to carry enough reserve so as to satisfy the following requirements: $-Imb_A \leq p_A - f, -Imb_B \leq p_B + f, p_A \leq r_A, p_B \leq r_B, -T \leq f \leq T$. Here, r_z is the amount of reserve in area z, p_z is the amount of balancing energy that is activated in area z, and f is the flow from link A to link B.

Exploiting symmetry, we can limit our consideration to the case where each area carries the same amount of reserve capacity, $r_A = r_B = r$. The space of imbalances can be partitioned into different regions, as indicated in Fig. 3. These can be described as follows:
(i) Region A (load is served): the line is not carrying reserve, $-Imb_A \leq r$, $-Imb_B \leq r$, with probability $\Phi_{\mu,\sigma}(r)^2$.
(ii) Region B (load is not served): the total imbalance exceeds available reserve, $-Imb_A - Imb_B \geq 2 \cdot r$, with probability $(1 - \Phi_{\mu,\sigma}(r))^2$.
(iii) Regions C and D (load is served): reserve is delivered from area B to area A (A to B respectively). This consists of two components: $r \leq -Imb_A \leq r + T, -Imb_B \leq r - T$, with probability $2 \cdot \Phi_{\mu,\sigma}(r - T) \cdot (\Phi_{\mu,\sigma}(r + T) - \Phi_{\mu,\sigma}(r))$. And $r \leq -Imb_A \leq r + T, r - T \leq -Imb_B \leq 2 \cdot r + Imb_A$, with probability $2 \cdot \int_{x=r}^{r+T} \phi_{\mu,\sigma}(x) \int_{y=r-T}^{2 \cdot r - x} \phi_{\mu,\sigma}(y) dy dx$.
(iv) Region E and F (load is not served): even though the system has enough reserve to cope with the total imbalance, the line cannot support its transfer. f

[8]Note that independence is only adopted as an assumption for the sake of the illustrative example of section II-A, and is not required for the generic model that is presented in section II-B or the solution methodology of section III.

[9]For these countries, the control area coincides with the LFC Block which coincides with the LFC area.

[10]This is referred to as *imbalance netting*. In reference to the previous fotonote, it is worth noting that the French, German and Belgian TSO ignore imbalance netting at the dimensioning stage.

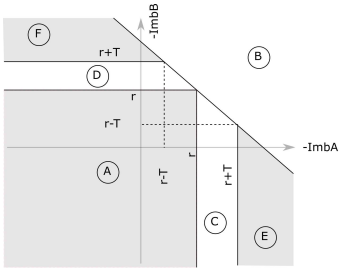

Fig. 3. Partition of the imbalance space to different regions, depending on whether imbalances can be covered or not, and depending on whether the transmission line of Fig. 2 is congested or not.

The probability of covering imbalances is then given by the sum of the probabilities of regions A, C, and D. We can plot this expression as a function of r, in order to find the smallest value of r that meets the target 99.9%. For $T = 80$ MW, each area should carry 252 MW, so the total reserve is 504 MW. Note that the existence of the line achieves some of the benefits of reserve sharing (the total reserve is less than 658.2 MW), but not all of them (if the areas were fully integrated the reserve requirement would drop down to 437 MW), because the line is occasionally congested. These significant potential savings are confirmed for the Swedish system in the case study of section IV.

The example serves two purposes: it elucidates the problem that we are interested in solving, and why existing probabilistic methods that rely on distributions [25], [9], [16] are hopeless for the task: the number of regions that need to be considered grows exponentially with the number of areas. Our analytical solution relies on a parametric distribution, it requires symmetry in order to reduce a two-dimensional problem to a one-dimensional problem, and it does not consider contingencies or the random availability of transmission capacity. Furthermore, it is unclear how this approach would be generalized to consider both upward and downward reserve. In the following section we overcome all of these challenges by proposing a chance-constrained formulation of the problem.

B. Chance-Constrained Formulation

We propose the following formulation for the sizing of reserves according to SOGL guidelines:

$$\min_{r^{+/-}\geq 0, l^{+/-}\geq 0, p, f, u^{+/-}\in\{0,1\}} \sum_{z\in Z} r_z^+ + \sum_{z\in Z} r_z^- \quad (1)$$

$$p_{zi} + l_{zi}^+ - l_{zi}^- + \Delta_{zi} + C_{zi} = \sum_{k=(z,\cdot)\in K} f_{ki} - \sum_{k=(\cdot,z)\in K} f_{ki}, z\in Z, i\in I \quad (2)$$

$$-r_z^- \leq p_{zi} \leq r_z^+, z\in Z, i\in I \quad (3)$$

$$l_{zi}^+ \leq \max(-\Delta_{zi} - C_{zi}, 0)\cdot u_i^+, z\in Z, i\in I \quad (4)$$

$$l_{zi}^- \leq \max(\Delta_{zi} + C_{zi}, 0)\cdot u_i^-, z\in Z, i\in I \quad (5)$$

$$T_{ki}^- \leq f_{ki} \leq T_{ki}^+, k\in K, i\in I \quad (6)$$

$$\sum_{i\in I} u_i^+ \leq (1-R^+)\cdot N, \sum_{i\in I} u_i^- \leq (1-R^-)\cdot N \quad (7)$$

The notation employed in the model is described in the appendix. The model is expressed as a two-stage stochastic mixed integer linear program. First-stage decisions $r^{+/-}$ correspond to zonal reserve capacities. Uncertainty (described by a set of scenarios I) is revealed in the form of continuous imbalances Δ, contingencies C, and transmission network capacities T. In the second stage, the program determines reserve activations p, implied flows f, and whether or not imbalances are covered $u^{+/-}\in\{0,1\}$. The objective expressed in Eq. (1) aims at minimizing the total upward and downward reserves. Eq. (2) corresponds to area power balance. Note that we employ a transportation-based model of the network[11], although the extension to a linear approximation of power flow is straightforward. Constraint (3) limits activated balancing energy between the downward and upward capacity of a given area. Conditions (4) and (5) introduce slack variables $l^{+/-}$ which are non-zero if and only if imbalances cannot be covered for a given realization. These slack variables can only be non-zero when the binary indicator variables $u^{+/-}$ are equal to 1 for a given scenario. Thus, if $u_i^{+/-} = 1$ for a given scenario i, it implies that imbalances cannot be covered in that scenario, for the given reserve sizing. Flow limits are imposed in constraint (6). Constraints (7) impose reliability limits for upward and downward reserves respectively. It is exactly these constraints that impose the mathematical condition that $\mathbb{P}$[negative/positive imbalance unserved] $\leq 1 - R^{+/-}$.

Intuitively, reserve sizing tends to be driven by samples in which the system is very long or very short, and these tend not to occur simultaneously. This suggests that it should be possible to arrive to high-quality results by considering upward and downward sizing independently. This would decrease the number of binary variables in problem (1)-(7) by half, and thus result in computational savings. It can formally be proven[12] that, if $\sum_{z\in Z} l_{zi}^{+,\star} \cdot \sum_{z\in Z} l_{zi}^{-,\star} = 0$ for all $i\in I$ in the optimal solution of the problem, then problem (1)-(7) can indeed be decomposed into a positive and a negative reserve dimensioning problem. It is further interesting to note that, although the condition of the above proposition is sufficient for guaranteeing decomposability, it is not necessary. However, if one chooses to decompose the reserve sizing problem, then it becomes unclear what input should be used for the remaining ATC capacities in the mFRR dimensioning problem of Fig. 5. For this reason, and since our proposed heuristic is capable of rapidly solving the problem even in large-scale instances, we retain the integrated optimization problem of Eqs. (1)-(7) in our case study in section IV.

Note that the input samples of the model can correspond to historical data or a simulator. Contingencies can be accounted for in the model as long as (i) they are present in the input historical data, or (ii) as long as they are sampled in a system simulator.

Setting the ATC capacities of Eq. (6) to $T_{ki}^+ = T_{ki}^- = 0$ corresponds to a pessimistic scenario of no coordination

[11]The transportation model is especially relevant in the context of the Swedish network, which extends from north to south and thus obeys a radial topology, see also Fig. 1.

[12]See section 1 of https://ap-rg.eu/wp-content/uploads/2021/11/J34AdditionalResults.pdf.

between LFC areas and provides an upper bound to the optimal solution. Setting the ATC capacities of Eq. (6) to $T^+_{ki} = -T^-_{ki} = +\infty$ corresponds to an optimistic copper-plate scenario and provides a lower bound to the optimal solution. These quantities are computed in the case study of section IV as a means of quantifying the potential benefit of our proposed model for the dimensioning of reserve requirements in Sweden.

III. Solution Methodology

A. Linear Relaxation Heuristic

The obvious drawback of the formulation of section II-B is that it is a large-scale mixed integer linear program. Moreover, it is interesting to note that constraints (7) couple scenarios *directly*. This should be contrasted to the L-shaped structure that is encountered more often in stochastic programs, where scenarios depend on each other only on account of their link to first-stage decisions. This structure precludes the straightforward application of dual decomposition methods that rely on the relaxation of non-anticipativity constraints and have proven to be successful in the context of other large-scale two-stage stochastic mixed integer linear programs [26], such as stochastic unit commitment [22].

An interesting alternative that can be contemplated for the application at hand is the scenario-based convex formulation of Calafiore [27]. Indeed, the model of section II-B can be cast in the format of [27] by defining second-stage cost as the sum of the slack variables $l^{+/-}$, which is a function of first-stage decisions and uncertainty realizations, and requiring this function to be non-negative. However, although [27] provides a link between the number of scenarios that can be used in the formulation of the problem and the probability of satisfying the reliability constraint, the approach fails to capture directly the tension between the probabilistic constraint and the objective of the problem.

The approach that we propose for solving the problem relies on solving the linear relaxation of the original problem (i.e. the MILP of section II-B), and using the solution of this linear relaxation as a means of recovering a reasonable feasible solution. The idea is specifically to rank the binary variables of the solution, and retain the ones whose value is closest to 1, as those scenarios for which the system should accept a "failure" in the sense of not being able to cover imbalances. We can then re-solve the remaining problem of finding what is the minimal level of reserve that can accommodate those scenarios for which we aim at balancing the system. The heuristic can thus be summarized as follows:

Step 1: Solve the linear relaxation of problem (1) - (7).

Step 2: Sort the variables $u^{+,\star}$ and $u^{-,\star}$ in decreasing order. Define I^+ as the set of scenarios corresponding to the $\lfloor (1 - R^+) \cdot N \rfloor$ most highly ranked variables $u_i^{+,\star}$ (analogously for $u_i^{-,\star}$).

Step 3: Re-solve the linear relaxation of problem (1) - (7) with the additional constraints[13] $u_i^+ = 1, i \in I^+$, $u_i^- = 1, i \in I^-$, $u_i^+ = 0, i \in (I^+)^c$ and $u_i^- = 0, i \in (I^-)^c$. Ties between scenarios at the cutoff can be broken arbitrarily.

Notice that the overall procedure amounts to solving two linear programs, and is therefore highly scalable with respect to the number of scenarios. On the other hand, our heuristic carries no guarantees regarding the quality of the furnished solution[14]. At the very least, the solution is guaranteed to be feasible. In the corner cases of zero and infinite inter-area capacity, the heuristic can be shown to be exact[15].

B. Minimizing Inter-Area Flows

Whereas large hydropower plants along with newly installed wind capacity in Sweden are concentrated in the north (largely SE1 and SE2, refer to Fig. 1), the main points of consumption (cities, industry) are located in the south (largely SE3 and SE4), and Sweden also tends to export energy to continental Europe. Carrying power through long distances results in the TSO being a major consumer of electricity, with losses representing approximately 7.5% of national consumption in recent years. Moreover, freeing up space on the largest corridors places the grid in a more favorable state during large disturbances, which to some extent explains the location of nuclear units in SE3. This motivates a criterion of sizing in a way that the exchange of balancing energy does not congest transmission lines.

One can approach this secondary goal by introducing an additional term in the objective function of (1) which penalizes inter-zonal flows resulting from the exchange of balancing energy. The drawback of such an approach is that it deteriorates the principal goal of keeping the procured reserve capacity as low as possible. Alternatively, we can use the heuristic of section III-A in order to identify a target level of upward and downward capacity for the entire control area, and then solve the following linear program in order to select among multiple solutions which can achieve the same total reserve capacity those solutions which minimize the total exchange of balancing energy:

$$\min_{l^{+/-} \geq 0, p, f, r^{+/-} \geq 0} \sum_{i \in I} \sum_{k \in K} |f_{ki}| \tag{8}$$

$$(2), (3), (6)$$

$$\sum_{z \in Z} r_z^- = \sum_{z \in Z} r_z^{-,\star}, \sum_{z \in Z} r_z^+ = \sum_{z \in Z} r_z^{+,\star} \tag{9}$$

$$l_{zi}^+ \leq \max(-\Delta_{zi} - C_{zi}, 0) \cdot u_i^{+,\star}, z \in Z, i \in I \tag{10}$$

$$l_{zi}^- \leq \max(\Delta_{zi} + C_{zi}, 0) \cdot u_i^{-,\star}, z \in Z, i \in I \tag{11}$$

Here, $r^{+,\star}$, $r^{-,\star}$, $u^{+,\star}$ and $u^{-,\star}$ correspond to the solutions that are obtained from the heuristic of section III-A.

The objective function (8) aims at minimizing the absolute value of inter-zonal flows caused by the balancing actions. Although absolute values are used here for brevity, it is straightforward to express this objective function as a linear

[13] Given a set A, we denote its complement by A^c.

[14] The heuristic has been observed to furnish a solution within 3.5% of the optimal MILP solution for an instance of the example of section II-A that consists of 1000 scenarios and a transmission capacity of 80 MW between the two areas.

[15] See section 2 of https://ap-rg.eu/wp-content/uploads/2021/11/J34AdditionalResults.pdf.

program. Constraint (9) ensures that the solution furnished in this step matches the level of reserves that is determined from the heuristic of section III-A.

Note that step 3 and the model of Eqs. (8) - (11) can be integrated into a single linear program using the optimality conditions of the linear program of step 3. As we demonstrate in section IV, the potential gains of such a merge would be limited to a few hundred seconds of run time for the realistic-scale instance that we consider in this paper. We therefore retain these two steps as separate optimization models in the case study of section IV.

C. Splitting Reserve between aFRR and mFRR

The splitting of FRR capacity between aFRR and mFRR has been investigated in detail in the European reserve sizing literature. The sizing of the two types of capacity is interdependent, for two reasons: (i) both capacities ultimately aim at eliminating the total system imbalance (we refer to this as *energy coupling*) and (ii) the flows induced by the activation of each of these reserves occupies the same transmission line capacity (we refer to this as *network coupling*).

An approach that is sometimes adopted in the literature is to preallocate specific imbalance drivers to specific types of reserves [28]. Another approach that is often applied in the literature is to size total FRR and one of the two reserve types, and then allocate the difference to the other reserve type. This is the case, for instance, in [5], [29] and [8], where the total FRR requirement is based on all sources of uncertainty, aFRR is sized in order to handle a subset of imbalance drivers, and mFRR is determined as the difference between total FRR and aFRR. Although these approaches account for the energy coupling of reserves, none of the methods accounts for network coupling.

In order to tackle energy coupling, we propose the procedure that is depicted in Fig. 4. The approach is similar in spirit to [30], where the authors size aFRR in order to balance noise related to load, which is defined as the deviation of load from its 15-minute average. The idea is to compute the component of the imbalance signal that mFRR targets to balance out as the 15-minute average of the 1-minute imbalance data that we have access to. We then generate imbalance scenarios for the aFRR sizing problem according to Fig. 4. For each 15-minute interval, we compute the five-minute moving average (blue curve) of the 1-minute imbalance (green curve) and the average 15-minute imbalance (orange curve). This is a proxy of the reactive aFRR setpoint. For each imbalance interval, we then measure the aFRR upward capacity as the maximum difference between the moving average and the 15-minute average (red arrows in Fig. 4), and the downward aFRR capacity as the minimum difference between the moving average and the 15-minute average (gray arrows in Fig. 4). We thus obtain one upward and one downward aFRR data point for each 15-minute imbalance interval. This procedure of computing input imbalance data aims at being representative of the physical sequence of reserve activations, and accounts for the proactive nature of mFRR activation and the reactive nature of aFRR activation. This is in contrast to alternatives for

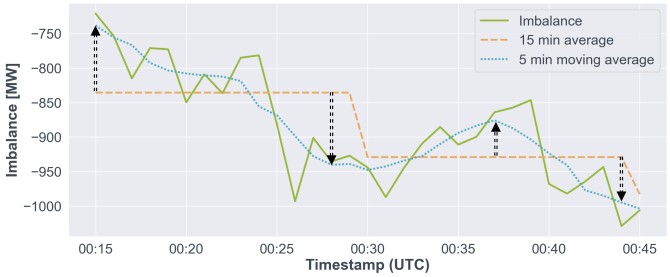

Fig. 4. Transformation of the minute-by-minute imbalance to a fast and a slow-moving component that are used for mFRR / aFRR splitting. The green curve is the system imbalance. The orange curve is the average over 15 minute imbalance intervals. The blue curve is the 5-minute moving average.

mFRR / aFRR splitting, such as a high-pass filter for isolating the fast component of the imbalance time series, which have been observed to under-commit aFRR capacity.

In order to tackle network coupling, we propose the procedure depicted in Fig. 5. The idea is to size mFRR capacity by assuming that the entire leftover network capacity (i.e. network capacity that is not contracted in the day-ahead or intraday markets) is available, since this reserve is proactively activated first. We then compute transmission capacity available for aFRR as the difference between original available transmission capacity (ATC) and the amount of capacity that is used as a result of mFRR activations. This is indicated in the middle blue box of Fig. 5. This is consistent with the reactive activation of aFRR and accounts for the amount of capacity that is used up by mFRR. Note that the overall procedure of Fig. 5 can be rearranged in order to match the specific balancing philosophy of different TSOs.

D. Overall Procedure

We close this section by summarizing the overall procedure that is depicted in Fig. 5. The procedure consists of solving the following sequence of problems:

1) One mixed integer linear program with annual input data, in order to determine the total mFRR reserve target for the system. This is indicated as the first box in the left of Fig. 5. We replace this MILP by a heuristic that solves the linear relaxation of Eq. (1) - (7) in order to determine which indicator variables u should be binary, followed by a linear program that solves Eq. (1) - (7) with u fixed, so as to determine the total mFRR reserve target, $\sum_{z\in Z} r_z^+$ and $\sum_{z\in Z} r_z^-$, in the system.
2) The linear program of Eqs. (8) - (11) with annual input data. This is indicated as the second box of Fig. 5. The output of this model is the spatial allocation of mFRR capacity in different LFC areas, $(r_z^+, r_z^-, z \in Z)$, and the flow along each interconnector, $(f_{ki}, k \in K, i \in I)$, which can be used in order to determine the leftover ATC capacity for the next step.
3) One mixed integer linear program with annual input data, in order to determine the total aFRR reserve target for the system. This is indicated as the third box of

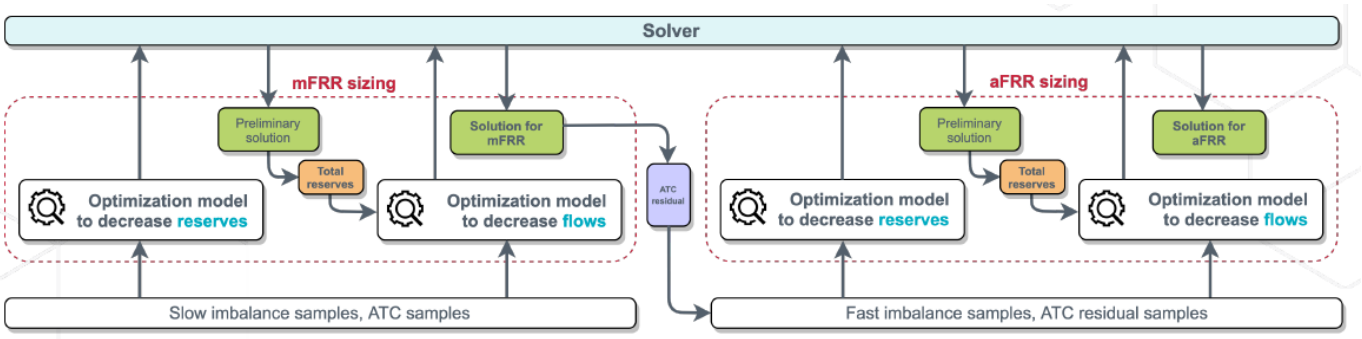

Fig. 5. The overall solution to the dimensioning problem which accounts for energy and network coupling of mFRR / aFRR capacities, and the minimization of inter-zonal flows.

Fig. 5. This is twice as large as the corresponding MILP of item 1, because the input data has twice the temporal resolution. As in the case of item 1, we replace this MILP by a heuristic that solves the linear relaxation of Eq. (1) - (7) in order to determine which indicator variables u should be binary, followed by a linear program that solves Eq. (1) - (7) with u fixed, so as to determine the total aFRR target, $\sum_{z\in Z} r_z^+$ and $\sum_{z\in Z} r_z^-$, in the system.

4) The linear program of Eqs. (8) - (11) with annual input data. This is indicated as the fourth box of Fig. 5. This model is twice as large as that of the second item, due to the fact that the input data has twice the resolution. The output of this model is the spatial allocation of aFRR in different LFC areas, $(r_z^+, r_z^-, z \in Z)$, as well as the flow along each interconnector, $(f_{ki}, k \in K, i \in I)$, which can be used in order to determine the leftover ATC capacity after balancing.

IV. Results

A. Preliminaries

We implement our proposed methodology on the problem of sizing reserve for the Swedish power system, with a target reliability of $R^+ = R^- = 99\%$. The data provided by the Swedish TSO includes 1-minute imbalance data, as well as ATC capacities with 1-hour resolution. We also have access to time stamps that correspond to imbalance intervals with significant frequency excursions (concretely, excursions beyond +/- 0.1 Hz), which we interpret as periods during which contingencies occur in the system[16].

We consider one year of input data for generating the N scenarios of our model, and in particular 2020. Since 2020 is a leap year, it corresponds to 366 days. We thus arrive to a model with N =35,136 scenarios for mFRR sizing (number of 15-minute intervals in a leap year) and N =70,272 scenarios for aFRR sizing (twice as many, since we have two data points per imbalance interval for aFRR sizing, as indicated in Fig. 4). The aFRR sizing model thus corresponds to 1,264,944 continuous variables, 140,544 binary variables, and 2,248,706 constraints. The linear relaxation heuristic of Fig. 5 requires 267 seconds for solving the LP relaxation of model (1) - (7) for aFRR sizing (step 1 of the heuristic of section III-A), and 115 seconds for solving the LP of step 3 of the heuristic of section III-A for aFRR sizing. The flow minimization model of section III-B requires 187 seconds. Simulations have been performed on a MacBook Pro with a 2.3 GHz 8-core Intel Core i9 processor on CPLEX 12.10. Launching the MILP directly on the same machine produces an optimality gap of 41.1% after 24 hours of run time. This demonstrates that the direct MILP formulation is not acceptable for problems of practical size.

B. Sizing Results

Before presenting the benefits of our proposed approach, we describe the procedures by which we estimate indicative lower and upper bounds on the total sizing results for $R = 99\%$. Lower bounding essentially corresponds to the copperplate ($T = +\infty$) paragraph of section II-A, and simply amounts to merging the imbalances of the four Swedish areas and ignoring the fact that the inter-zonal ATC capacity is limited. Upper bounding corresponds to the "no reserve sharing" ($T = 0$ MW) paragraph of section II-A, and amounts to solving[17] the following non-liner equation with respect to r: $\mathbb{P}[\max(Imb_z) \leq r] = R$, which gives the reserve need for area z. Assuming independent imbalances between LFC areas, this equation can be re-expressed as $\Pi_{z=1}^4 \mathbb{P}[Imb_z \leq r] = R$. Note that we assume an equal allocation of reserve in each area in computing the upper bound, which is valid, since this is a feasible but not necessarily optimal reserve allocation.

The upward and downward FRR results are presented in Table I. The total upward capacity amounts to 1611 MW. The upper bound is 3356 MW, while the lower bound is 1109 MW,

[16]We choose to merge normal imbalances and contingencies in a single total imbalance signal $\Delta_{zi} + C_{zi}$. An alternative approach for capturing the interaction between normal imbalances and contingencies is to remove the imbalances corresponding to significant frequency excursions from the total imbalance data in order to isolate normal imbalances, and to simulate imbalances using forced outage rates. This approach would only be meaningful if the scenario size N of the input to the model of section II-B can be large enough to capture dimensioning incidents with their representative frequency of occurrence. An alternative that is commonly employed in practice for copperplate sizing is to include the N-1 dimensioning incident as a lower bound of the sizing solution.

[17]Since $\mathbb{P}[\max(Imb_z) \leq r]$ is a monotonically increasing function of r, we can solve this equation graphically or through bisection.

TABLE I
ALLOCATION OF UPWARD AND DOWNWARD FRR CAPACITY IN SWEDISH AREAS, AND COMPARISON TO LOWER AND UPPER BOUNDS. ALL REPORTED VALUES ARE IN MW.

	Upward	Downward
SE1	126	454
SE2	60	922
SE3	611	85
SE4	814	108
Total	1611	1569
Lower bound	1109	1053
Upper bound	3356	3216

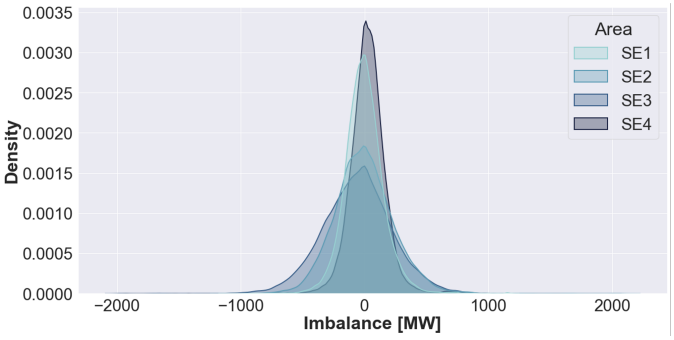

Fig. 6. Empirical probability density functions of the imbalances in each Swedish area for the data of 2020.

which means that a sharing methodology can reduce reserve requirements by up to 2247 MW. As our sizing methodology achieves savings of 1745 MW out of these potential savings, we thus conclude that our methodology captures 77.7% of the potential savings of a copperplate solution. Analogously, the total downward capacity determined by our method amounts to 1569 MW. The lower bound is 1053 MW, while the upper bound is 3216 MW. We thus capture 1647 MW out of 2163 MW, or 76.1% of the potential savings of a copperplate solution[18].

In order to gain intuition about the spatial allocation of reserves in table I, we point out two observations: (i) Upward and downward imbalances in areas SE2 and SE3 are the most severe, as indicated in Fig. 6. (ii) As indicated previously, power is typically transported from north to south. Consequently, the inter-zonal links SE2-SE3 and SE3-SE4 are typically the ones with the least available capacity, as indicated in Fig. 7. Thus, for central Sweden (SE2 and SE3) to source upward balancing energy, it would be necessary to rely on reserves in the south, since the SE2-SE3 corridor hinders balancing energy from being delivered to SE3[19]. Symmetrically, in order for central Sweden to evacuate downward balancing energy, it would need to rely on downward balancing capacity in the north, so that the evacuated power is moved opposite

[18]It is worth noting that applying our heuristic to the problem without constraints (6) results in the same amount of total reserve capacity as the heuristic *with* the transmission constraints enforced, but with the capacity being more evenly divided between areas.

[19]The reader is referred to the discussion in the end of section IV-B about how the results of the model compare to the existing spatial allocation of reserve in Sweden.

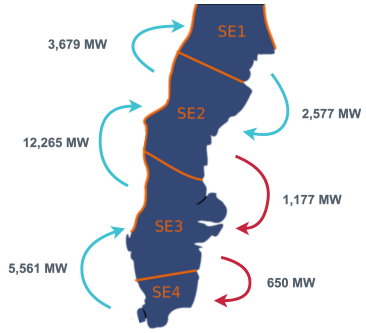

Fig. 7. Average ATC capacity for each link of the Swedish system over the data of 2020. Note that SE2-SE3 and SE3-SE4 are the most congested corridors, and are thus indicated in red.

to the direction of the congestion. This is exactly the pattern that is observed in Table I.

The split of reserve capacity between aFRR and mFRR is presented in Fig. 8. The geographical allocation of the aFRR and mFRR capacities follows the trend of the total FRR, with more upward aFRR / mFRR capacity located in the south, and more downward aFRR / mFRR capacity located in the north. We note that the total aFRR capacity is consistent with the recommended minimum aFRR capacity according to the methodology of the former Union for the Coordination of Transmission of Electricity (UCTE), as indicated in Fig. 6 of the Synchronous Area Framework Agreement [31]. Concretely, the peak load of Sweden slightly exceeds 25 GW, which maps to approximately 400 MW of aFRR according to Fig. 6 of [31]. Note, however, that the latter method does not prescribe how this aFRR capacity should be distributed throughout the network.

In Table II we present the congestion of the system after implementing the sizing decision of Table I. Note that the links that are not presented in the table (SE2→SE1, SE3→SE2, and SE4→SE3) exhibit no congestion. We consider a link as being congested when the leftover capacity in the link is no greater than 100 MW. Recall from Fig. 5 that mFRR capacity is sized first, followed by aFRR capacity. It is thus possible to measure leftover transmission capacity[20] after sizing mFRR (column 3 of Table II), followed by transmission capacity after sizing aFRR (column 4 of Table II). We conclude that the allocation of reserves is such that balancing causes almost no additional congestion to the system. This behavior is consistent with the objective function (8) of the model of section III-B, which aims at minimizing inter-area flows due to balancing actions.

It is interesting to point out that the spatial allocation of reserve in the solution of the model differs from the existing allocation of reserve in Sweden. For instance, many of the reserves used for balancing the Swedish power system

[20]The models whose output $f^{\star}_{ki}$ is used for determining the flow that ultimately occurs in the system as a result of activating reserves are the optimization models for decreasing flows in Fig. 5. The condition for deciding that congestion has occurred along link k for scenario i is that $|T^{+}_{ki} - f^{\star}_{ki}| \leq 100$ MW, or $|T^{-}_{ki} - f^{\star}_{ki}| \leq 100$ MW.

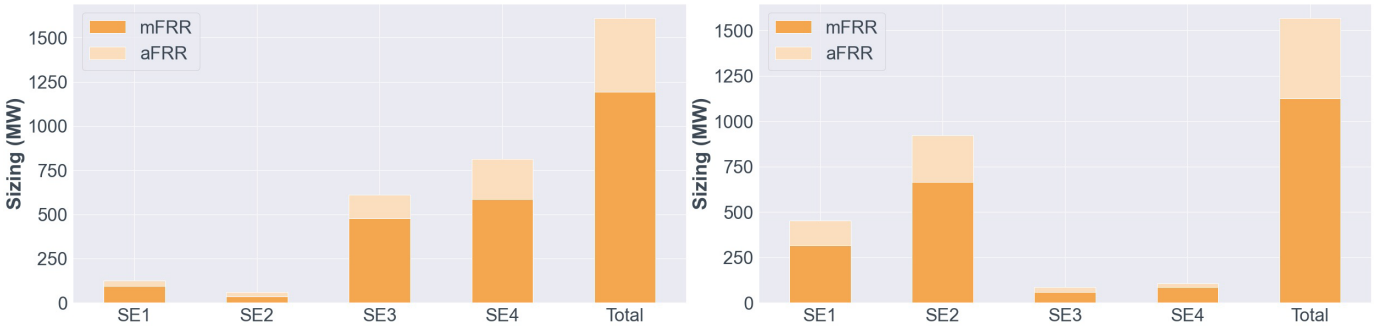

Fig. 8. The sizing results for FRR capacity in the upward (left) and downward (right) direction.

TABLE II
PROBABILITY OF CONGESTIONS BEFORE AND AFTER SIZING FOR LINKS THAT EXHIBIT CONGESTION. WE CONSIDER A LINK AS BEING CONGESTED WHENEVER THE LEFTOVER CAPACITY ON THE LINK IS NO GREATER THAN 100 MW.

Link	Before sizing	After mFRR sizing	After aFRR sizing
SE1→SE2	0.1	0.1	0.1
SE2→SE3	38.2	38.2	38.2
SE3→SE4	43.9	44.0	44.0

today are hydro plants which are located in the north. The generalization of our proposed model and solution algorithm in order to consider alternative criteria (including an objective function based on cost, or the fact that certain reserve resources are already in place) is straightforward from a modeling standpoint.

C. Additional Sensitivities

An important attribute of the method is stability, in the sense of arriving to the same result for different scenarios. In order to examine this behavior, we report the sizing results as a function of the number of scenarios N that are used as input for the model in Fig. 9. Concretely, as we move further along the x axis in the figure, we are looking deeper into the "past" of the historical data: for $x = 1$ we are only sizing given the results of the first 15 minutes of 2020, while for $x = 35,136$ we are taking into consideration the full year of 2020. We observe that the total sizing result stabilizes around 1700 MW for both upward and downward reserves after four months of data are accounted for. Nevertheless, the distribution among areas is highly influenced by the available transfer capacity, as we can observe in the evolution of reserves in SE3 and SE4. The shift in the capacity of SE3 and SE4 in the left panel of the figure can be attributed to a significant drop in the available ATC of the SE3→SE4 link during the autumn of 2020.

The sizing results as a function of an increasing reliability target are presented in Fig. 10. Note that Fig. 10 is plotted by running the *full* year of 2020 data for different levels of target reliability. It is worth noting that the precise reliability targets that are considered in reserve sizing analyses are typically in the 99.x% level, and depend on assumptions about what each type of reserve is responsible for (e.g. contingencies or specific sources of continuous imbalances). We note that the total requirement increases rapidly as we approach a target reliability level of 100%, which reflects the significant influence of tail uncertainty in the sizing of reserves.

D. Practical Implementation Aspects

We consider a context of static dimensioning in the current work. The sizing procedure timeline is illustrated in Fig. 11. Note that historical input data is collected for the entire interval that the sizing decision is intended to protect against. This sizing process is executed once every year according to the timeline of Fig. 11, using the data of the past year. Although the diagram indicates an annual sizing, other intervals (e.g. quarterly) could be envisioned.

An important practical implementation aspect relates to the entity that would be responsible for executing the required sizing function. Various options may be considered, depending on the desired degree of decentralization, and we shortly comment on three such options and their relation to relevant EU legislation.

Option 1: independent computations (decentralized). Insofar as the Nordics are concerned, the Nordic TSOs have a strong collaboration, and regularly exchange all the data that is required for the proposed sizing model (imbalance data and ATC data) in the context of various joint projects. This implies that all of the Nordic TSOs could in principle run the full optimization independently, within a SCADA or near to SCADA setting.

Option 2 (centralized): rotating responsibilities. A more central calculation can save time that would be required for handshaking between the TSOs. It would then be interesting to consider an option of appointing a TSO within this multi-area setting, which would be responsible for the task of dimensioning. This can be achieved using a rotating schedule, and changing TSOs every year or every two years, for instance. Article 157(3) of the System Operation Guideline [4] indicates how this is to be implemented in a multi-area setting, and states that it needs to be a part of the LFC block operating agreement.

Option 3 (centralized): regional coordination centers. The LFC block cooperation agreement for the Nordics [32] indicates that the dimensioning methodology should be executed by a "common service provider". Such a common service provider could be a regional coordination center. Such a

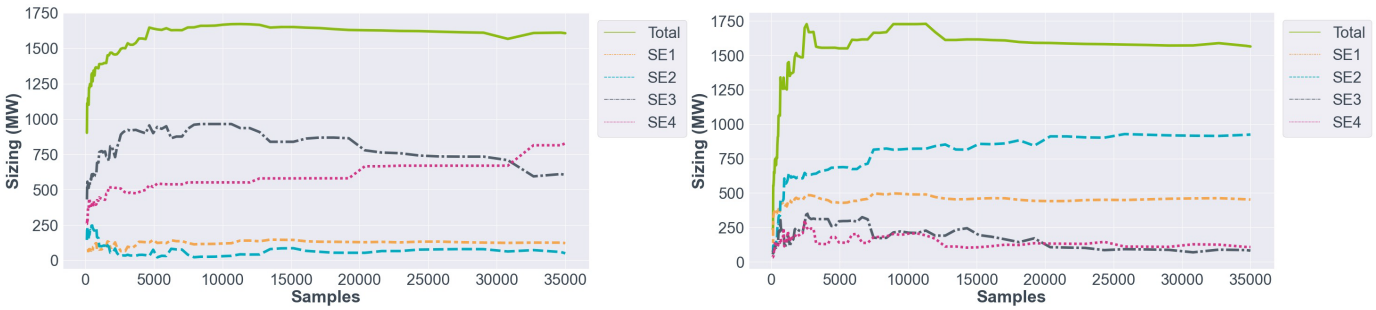

Fig. 9. The sizing results for FRR capacity in the upward (left) and downward (right) direction as a function of the number of input scenarios.

Fig. 10. The upward (left) and downward (right) reserve capacity as a function of an increasing reliability target.

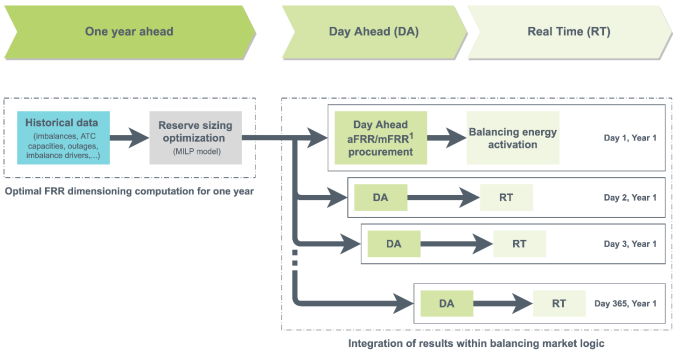

Fig. 11. Sizing procedure timeline where reserve is sized annually.

solution could extend beyond the Nordics, since regional coordination centers throughout Europe are intended to cover the regional needs of inter-TSO coordination throughout Europe.

V. Conclusion and Perspectives

In this article we present a novel model, methodology, and functioning application for the problem of sizing reserves subject to probabilistic requirements in a multi-area context where reserve sharing is foreseen.

In future work, we are interested in exploring tight formulations of chance constraints in order to attempt a direct resolution of the chance-constrained model without resorting to heuristics. We are further interested in the extension of the methodology to the entire Nordic system, as well as in the context of dynamic reserve dimensioning [9] where reserve requirements are adapted on a daily basis based on forecast system conditions in the day-ahead time frame.

The extension of the model so as to represent cost information related to the sourcing of reserve or minimum reserve requirements per LFC area (which could be interpreted as reserve capacity which is already installed in the corresponding LFC areas) is a straightforward extension of the existing model, and does not affect the implementation of the proposed heuristic. There is also an interesting institutional dimension of how one would evaluate the incremental cost of sourcing balancing capacity from different LFC areas, since this incremental cost would strongly influence the spatial allocation of reserve.

Appendix

In this section we present the notation that is used in the models of sections II-B and III-B, as well as the meaning of various abbreviations that are used throughout the text.

Sets

Z: set of LFC areas
K: set of links
$I = \{1, \ldots, N\}$: set of scenarios

Variables

$r_z^{+/-}$: upward/downward balancing capacity in zone z
$l_{zi}^{+/-}$: upward/downward failure-to-serve slack in zone z for scenario i
p_{zi}: balancing energy in zone z for scenario i
f_{ki}: flow on link k in scenario i
$u_i^{+/-}$: binary variable indicating failure to serve negative/positive imbalances

Parameters

$R^{+/-}$: Acceptable reliability for upward/downward balancing capacity
$T_{ki}^{+/-}$: Upward ATC capacity of link k in scenario i
Δ_{zi}: Normal imbalance of zone z for scenario i
C_{zi}: Contingency capacity of zone z for scenario i

Abbreviations
ACE: Area Control Error
aFRR: automatic Frequency Restoration Reserve
ATC: Available Transfer Capacity
FCR: Frequency Containment Reserve
FRR: Frequency Restoration Reserve
LFC: Load Frequency Control
LP: Linear Program / Programming
MARI: Manually Activated Reserves Initiative
MILP: Mixed Integer Linear Program / Programming
mFRR: manual Frequency Restoration Reserve
PICASSO: Platform for the International Coordination of Automated Frequency Restoration and Stable System Operation
RR: Replacement Reserve
SOA: System Operation Agreement
SOGL: System Operation Guideline
TSO: Transmission System Operator
UCTE: Union for the Coordination of Transmission for Electricity

REFERENCES

[1] European Commission, "Commission regulation (EU) 2017/2195 of 23 November 2017 establishing a guideline on electricity balancing," *Official Journal of the European Union*, 2017.

[2] T. Zheng and E. Litvinov, "Contingency-based zonal reserve modeling and pricing in a co-optimized energy and reserve market," *IEEE transactions on Power Systems*, vol. 23, no. 2, pp. 277–286, 2008.

[3] Y. Chen, P. Gribik, and J. Gardner, "Incorporating post zonal reserve deployment transmission constraints into energy and ancillary service co-optimization," *IEEE Transactions on Power Systems*, vol. 29, no. 2, pp. 537–549, 2013.

[4] European Commission, "Commission regulation (EU) 2017/1485 of 2 August 2017 establishing a guideline on electricity transmission system operation," *Official Journal of the European Union*, 2017.

[5] M. Bucksteeg, L. Niesen, and C. Weber, "Impacts of dynamic probabilistic reserve sizing techniques on reserve requirements and system costs," *IEEE Transactions on Sustainable Energy*, vol. 7, no. 4, 2016.

[6] D. Chattopadhyay and R. Baldick, "Unit commitment with probabilistic reserve," in *2002 IEEE Power Engineering Society Winter Meeting. Conference Proceedings (Cat. No. 02CH37309)*, vol. 1, 2002, pp. 280–285.

[7] A. Ohsenbrugge and S. Lehnhoff, "Dynamic dimensioning of balancing power with flexible feature selection," in *23rd international conference on electricity distribution*, 2015.

[8] D. Jost, A. Braun, R. Fritz, and S. Otterson, "Dynamic sizing of automatic and manual frequency restoration reserves for different product lengths," in *2016 13th International Conference on the European Energy Market (EEM)*, 2016.

[9] K. De-Vos, N. Stevens, O. Devolder, A. Papavasiliou, B. Hebb, and J. Matthys-Donnadieu, "Dynamic dimensioning approach for operating reserves: Proof of concept in Belgium," *Energy Policy*, vol. 124, pp. 272–285, 2019.

[10] B. Park, Z. Zhou, A. Botterud, and P. Thimmapuram, "Probabilistic zonal reserve requirements for improved energy management and deliverability with wind power uncertainty," *IEEE Transactions on Power Systems*, vol. 35, no. 6, pp. 4324–4334, 2020.

[11] Nordic TSOs. (2019) Nordic system operation agreement (SOA) - annex load-frequency control & reserves (LFCR). [Online]. Available: https://eepublicdownloads.entsoe.eu/clean-documents/SOC%20documents/Nordic/Nordic%20SOA_Annex%20LFCR.pdf

[12] ——. (2019) Amended Nordic synchronous area proposal for the FRR dimensioning rules in accordance with Article 157(1) of the Commission Regulation (EU) 2017/1485 of 2 August 2017 establishing a guideline on electricity transmission system operation. [Online]. Available: https://www.svk.se/siteassets/press-och-nyheter/nyheter/inlamnade-och-godkanda-forslag-natkoder/190513-frr-dimensioning-rules-final.pdf

[13] ——. (2019) Explanatory document for the amended Nordic synchronous area proposal for the FRR dimensioning rules in accordance with Article 157(1) of the Commission Regulation (EU) 2017/1485 of 2 August 2017 establishing a guideline on electricity transmission system operation. [Online]. Available: https://www.svk.se/siteassets/press-och-nyheter/nyheter/inlamnade-och-godkanda-forslag-natkoder/190513-explanatory-document-for-frr-dimensioning-rules-final.pdf

[14] J. R. Birge and M. A. H. Dempster, "Stochastic programming approaches to stochastic scheduling," *Journal of Global Optimization*, vol. 9, no. 3-4, pp. 417–451, 1996.

[15] C. Singh, P. Jirutitijaroen, and J. Mitra, *Electric power grid reliability evaluation: models and methods*. John Wiley & Sons, 2018.

[16] J. De Haan, M. Gibescu, D. Klaar, and W. Kling, "Sizing and allocation of frequency restoration reserves for LFC block cooperation," *Electric Power Systems Research*, vol. 128, pp. 60–65, 2015.

[17] J. D. Lyon, K. W. Hedman, and M. Zhang, "Reserve requirements to efficiently manage intra-zonal congestion," *IEEE Transactions on Power Systems*, vol. 29, no. 1, pp. 251–258, 2013.

[18] F. Wang and Y. Chen, "Market implications of short-term reserve deliverability enhancement," *IEEE Transactions on Power Systems*, vol. 36, no. 2, pp. 1504–1514, 2021.

[19] M. Vrakopoulou, K. Margellos, J. Lygeros, and G. Andersson, "A probabilistic framework for reserve scheduling and N-1 security assessment of systems with high wind power penetration," *IEEE Transactions on Power Systems*, vol. 28, no. 4, pp. 3885–3896, 2013.

[20] L. Roald, S. Misra, T. Krause, and G. Andersson, "Corrective control to handle forecast uncertainty: A chance constrained optimal power flow," *IEEE Transactions on Power Systems*, vol. 32, no. 2, pp. 1626–1637, 2016.

[21] M. A. Bucher, M. A. Ortega-Vazquez, D. S. Kirschen, and G. Andersson, "Robust allocation of reserves considering different reserve types and the flexibility from HVDC," *IET Generation, Transmission & Distribution*, vol. 11, no. 6, pp. 1472–1478, 2017.

[22] A. Papavasiliou and S. S. Oren, "Multi-area stochastic unit commitment for high wind penetration in a transmission constrained network," *Operations Research*, vol. 61, no. 3, pp. 578–592, May / June 2013.

[23] Y. Zhang, J. Wang, B. Zeng, and Z. Hu, "Chance-constrained two-stage unit commitment under uncertain load and wind power output using bilinear Benders decomposition," *IEEE Transactions on Power Systems*, vol. 32, no. 5, pp. 3637–3647, 2017.

[24] ELIA. (2020) Methodology for the dimensioning of the aFRR needs: public consultation. [Online]. Available: https://www.elia.be/en/public-consultation/20200602_public-consultation-on-the-methodology-for-the-dimensioning-of-the-afrr-needs

[25] ELIA, "Tariffs for maintaining and restoring the residual balance of individual access responsible parties 2020-2023," Belgian Transmission System Operator, Tech. Rep., 2019.

[26] I. Aravena and A. Papavasiliou, "Asynchronous lagrange scenario decomposition," *Mathematical Programming Computation*, vol. 13, no. 1, pp. 1–50, 2021.

[27] G. Calafiore and M. Campi, "Uncertain convex programs: randomized solutions and confidence levels," *Mathematical Programming A*, vol. 102, pp. 25–46, 2005.

[28] S. Kippelt, T. Schlüter, and C. Rehtanz, "Flexible dimensioning of control reserve for future energy scenarios," in *2013 IEEE Grenoble Conference*, 2013.

[29] D. Jost, M. Speckmann, F. Sandau, and R. Schwinn, "A new method for day-ahead sizing of control reserve in germany under a 100% renewable energy sources scenario," *Electric Power Systems Research*, vol. 119, pp. 485–491, 2015.

[30] C. Breuer, C. Engelhardt, and A. Moser, "Expectation-based reserve capacity dimensioning in power systems with an increasing intermittent feed-in," in *2013 10th International Conference on the European Energy Market (EEM)*, 2013.

[31] Regional Group Contintental Europe. Synchronous Area Framework Agreement (safa) for Regional Group Continental Europe. annex I: Policy on Load-Frequency Control and reserves. [Online]. Available: https://download.terna.it/terna/Allegato%201_8d813a8e31e478b.pdf

[32] Affärsverket Svenska kraftnät, Energinet, Fingrid Oyj, Kraftnät Aland Ab, Statnett SF. (2018) Cooperation agreement, Nordic balancing

cooperation. [Online]. Available: http://nordicbalancingmodel.net/wp-content/uploads/2018/09/cooperation-agreement-incl-annexes.pdf

Anthony Papavasiliou (M'06-SM'20) is an Associate Professor at the Center for Operations Research and Econometrics at the Université catholique de Louvain, where he holds the ENGIE Chair. He works on operations research, electricity market design, and electric power system operations. He is the recipient of the Francqui Foundation research professorship (2018), the ERC Starting Grant (2019), and the Bodossaki Foundation Distinguished Young Scientist award (2021). He is an Associate Editor of Operations Research and the IEEE Transactions on Power Systems.

Alberte Bouso is an Energy Analytics Consultant at N-SIDE, where he has been working since 2020. He works on applications of mathematical programming and machine learning within electric power system operations. He holds a double master degree in Energy Engineering from the Royal Institute of Technology in Stockholm (KTH) and Catholic University of Leuven (KU Leuven).

Senad Apelfröjd received his M.Sc. in Energy Systems Engineering and Ph.D. degrees in Engineering Science with specialization in the Science of Electricity from Uppsala University, Uppsala, Sweden, in 2010 and 2016, respectively. He is currently with Svenska Kraftnät (Swedish National Grid), Department of Business Intelligence. His research interests include the area of real-time data and real-time applications in Supervisory Control and Data Acquisition (SCADA).

Ellika Wik received her M.Sc. in Energy Systems Engineering from Uppsala University, Uppsala, Sweden, in 2017. She is currently with Svenska Kraftnät (Swedish National Grid), Department of Power Systems. She works as a power system analyst focusing on frequency stability in power systems, including dimensioning of reserves and development of technical requirements for reserves.

Thomas Guening is a senior consultant at N-SIDE. He holds a master's degree in mathematical engineering from UCLouvain and a PhD on business statistics from KULeuven. He works on advanced analytics solutions for the energy sector, based on machine learning and mathematical optimization techniques. He notably contributes to Euphemia (European Single day-ahead Coupling algorithm) and reserve dimensioning topics.

Yves Langer holds a master in Business Engineering from HEC Lige (2003) and a DEA in Management Sciences (2005). He has more than 15 years of experience working on power market design topics, and currently advises market and system operators as a freelance consultant. Yves also acts as a senior market design expert for N-SIDE, where he mostly focuses on balancing markets and congestion management.